PERFORMANCE OF A REMOTE RAMAN SYSTEM: DEFINING REMOTE RAMAN EFFICIENCY.

J. D. Stopar[1, 2], P. G. Lucey[1], S. K. Sharma[1], H. W. Hubble[1], and A. K. Misra[1], [1]Hawaii Institute of Geophysics and Planetology, University of Hawaii (1680 East-West Rd., Honolulu, HI, 96822), [2]jstopar@hipg.hawaii.edu.

Introduction: Raman analysis is a concept that has been explored for many years [1-2]. Wang et al. first hypothesized on the usefulness of *in situ* Raman analysis for planetary landers [3] and later Jolliff et al. [4] among others. However, the applicability of a remote Raman system on planetary landers has only been investigated in the last few years [2], [5-8]. A proof-of-concept study conducted by Lucey et al. [5] showed that mineral spectra could be detected up to a distance of 10 meters. Initial tests of the system were conducted on earlier systems and equipment including preliminary calibration methods [6-8], however, the system is only now being refined through advancements in available equipment and analysis.

Landers and rovers have become increasingly important to solar system exploration, and we are designing and analyzing a remote Raman system to assess its applicability on a planetary mission. First, in order to design a flight instrument, the quantitative Raman efficiency of natural surfaces must be understood. While some Raman cross-sections on a per molecule basis are available [9-10] for compounds like benzene, the number is limited and the relationship to measured Raman efficiency of a rock surface is complex and has not been studied theoretically.

The remote Raman efficiency is a dimensionless quantity that we define here as the ratio of the irradiance (W/cm²) of the incident laser light to the Raman irradiance emitted from a surface. The irradiance of the surface is calculated from the measured absolute radiance of the Raman signal using an absolutely calibrated spectrometer and the spectral bandwidth of the spectrometer, and we assume isotropic scattering.

Equipment: Modern Raman systems use a laser as the excitation source, and our system employs a pulsed 532 nm ULTRA CFR Big Sky Nd:YAG Laser with 8 ns pulse width, repetition rate of 20 Hz, and 35 mJ/pulse power. We use mirrors to align the laser beam with the optic axis of the telescope in order to minimize the angle difference. The 5" telescope is an f/15 Meade ETX-125 Maksutov-Cassegrain. Light is transmitted through a series of lenses and a holographic notch filter mounted at the back of the telescope. The holographic notch filter is designed to reject reflected laser light from the collected spectra. The beam is further transmitted by a fiber optic that collects the light at the end of the optical system and redirects it to the spectrometer. This optical interface (lenses and fiber optic) is necessary in order to increase the amount of signal received by the spectrometer, which functions at an f/2.2 level. The spectrometer we employed is a HoloSpec f/2.2 with a 50-micrometer slit and an intensified CCD detector. Data was acquired in CW mode and collected in a dark room to decrease background noise. Data was acquired approximately 10 meters distance from the sample.

Samples: Rocks and minerals were acquired from Ward's Natural Science Establishment, Inc., Rochester, NY. The following were analyzed: milky quartz (University Rock-Forming Mineral Collection 45-0355 #46) from Fremont County, CO (Figure 1); dolomite marble (Ward's Collection of Classic North American Rocks 45-7250 #73) from Essex Count, NJ; dacite (45-7250 #26) from the Helena area, MT; rhyolite (45-7250 #11) from Castle Rock, CO; anorthosite (45-7250 #32) from Elizabethtown, NY; basalt (45-7250 #36) from Helena, MT; hornblende andesite (45-7250 #27) from Mineral County, NV; obsidian (45-7250 #8) from Lake County, OR; pumice (45-7250 #9) from Millard County, UT; epidote (45-0355 #31) from Calumet, CO; and micaceous hematite (45-0355 #71) from Republic, MI. We used a benzene sample in a glass container for wavelength calibration. One second integration time was used for the very Raman-active benzene sample, while rock samples were integrated for times between 30 seconds and 10 minutes in order to obtain a high SNR (Signal to Noise Ratio).

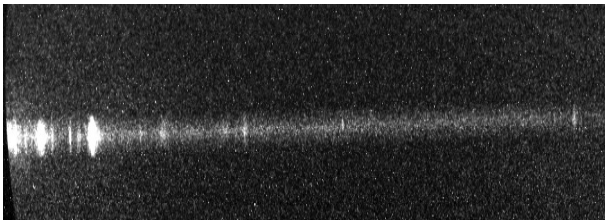

Figure 1: Spectral image of quartz, integration time is 30 sec.

All spectra collected contained some noise, and a noise reduction routine drastically increased the SNR. This process determined peak maxima and minima on spectral images and then binned intensity data acquired only from within this range in the spectral lines. A wavelength calibration was performed using our benzene spectrum and a spectrum for a known luminant source (an integrating sphere).

Remote Raman Efficiency: We define the remote Raman efficiency as the ratio of sample Raman irradiance (W/cm²) to incident laser irradiance (W/cm²).

Sample Raman irradiance is acquired by measuring the absolute radiance of the Raman signal for each sample and correcting for the solid angle, assuming isotropic scattering, and the spectral bandwidth of the spectrometer. Furthermore, the incident laser irradiance is calculated by finding the laser power (mW) from the laser pulse power and frequency, then dividing by the area of the laser spot on the sample. The remote Raman efficiency equation is as follows:

$$\frac{I_R}{I_L} = \frac{L_R \bullet \Omega \bullet \Delta\lambda}{E \bullet \left(N/A \right)}$$

where,
I_R = Raman irradiance of sample (W/cm²),
I_L = Irradiance of incident laser light (W/cm²),
L_R = Radiance of sample minus background ($Wcm^{-2}sr^{-1}nm^{-1}$),
Ω = angle in steradians (π sr),
$\Delta\lambda$ = spectral bandwidth of spectrometer (nm),
E = energy of laser (mJ/pulse),
N = pulse rate (Hz),
A = area of laser spot (cm²).

Results: We examined our rock and mineral spectra for characteristic Raman peaks. While the darker rocks did not produce enough Raman signal that could be isolated, three samples did produce spectra with significant peaks: quartz, dolomite marble, and anorthosite. Typical quartz spectra are shown in Figs. 2-3 (shown in absolute wavelength scale). The calculated remote Raman efficiency for each sample's strongest spectral peak are as follows: quartz = 9.5 x 10^{-8}, dolomite marble = 3.5 x 10^{-8}, and anorthosite = 3.0 x 10^{-9}.

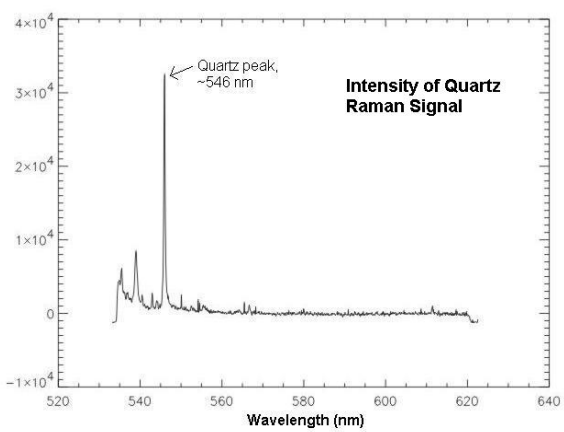

Figure 2: Raman spectrum of quartz sample, background has been removed, intensity units are arbitrary, quartz peak at ~546 nm (Note: absolute wavelength scale).

Applications of a Remote Raman System: In the future, we will continue efforts to make our Raman system lander-ready. Since Pathfinder has opened a new niche for exploratory and analytical technologies on planetary missions through the use of a rover to collect data [11], we envision many applications of a remote Raman system. Raman analysis onboard a lander or rover could provide detailed mineralogical data and can be combined with LIBS [12] to provide complementary elemental data.

Current landers employ XRF, thermal analysis, and mass spectrometry to acquire detailed compositional data. However, XRF requires close physical contact with the sample, while both thermal analysis and mass spectrometry require sample acquisition. Furthermore, Visible, Near-IR, and Thermal-IR spectra all have broad overlapping band features that can be difficult to interpret, while Raman bands are very narrow and distinct. At the very least, remote Raman analysis could be used to acquire data from numerous candidates and identify significant specimens for further analysis by the lander or rover, augmenting current imaging methods and possibly even replacing remote multi-spectral analysis. Remote Raman analysis onboard a lander or rover might potentially eliminate the need to manipulate surface rocks with complicated machinery or to maneuver a rover around impassible, rugged terrain.

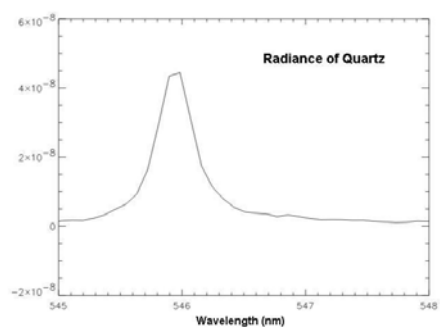

Figure 3: Raman radiance of quartz peak ($Wcm^{-2}sr^{-1}nm^{-1}$).

References: [1] Angel S. M. et al. (1992) *Appl. Spectrosc.,* 1085-1091. [2] Horton K. A. et al. (2001) *LPS XXXII,* Abstract #1462. [3] Wang et al. (1995) *JGR, 100,* 21189-21199 [4] Jolliff et al. (1999) *LPS XXX*, Abstract #1529 [5] Lucey P. G. et al. (1998) *LPS XXIX*, Abstract #1354. [6] Sharma S. K. et al. (2002) *Appl. Spectrosc.*, 699-705. [7] Horton K. A. et al. (2000) *LPS XXXI*, Abstract #1514. [8] Sharma S. K. (2001) *LPS XXXII*, Abstract #2066. [9] Eysel, H. et al. (1988) *J. Raman Spectrosc.*, 59-64. [10] Ray, K. et al. (1997) *Applied Spectrosc.,* 108-116. [11] Golombek M. P. et al. (1999) *JGR, 104,* 8523-8553. [12] Weins R. C. et al. (2000) *LPS XXXI*, Abstract #1468.